

## The initial development of longitudinal dispersion in straight tubes

By P. C. CHATWIN

Department of Applied Mathematics and Theoretical Physics,  
University of Liverpool

(Received 21 September 1976)

When a contaminant molecule is released in a laminar flow in a straight tube its motion differs from that of the fluid particle with which it initially coincided because of its random motion, whose intensity is measured by the molecular diffusivity  $\kappa$ . For  $T = \kappa t/a^2 \geq 0.25$ , where  $t$  is the time after release and  $a$  is a length characteristic of the cross-section, the statistics of its motion can be determined in the way described by Taylor (1953), Aris (1956) and Chatwin (1970). However, in many applications, including blood flow, the values of  $T$  which are attained are much smaller, and the purpose of this paper is to present first approximations for  $T \ll 1$  to some of the statistics measuring the deviations between the motion of the molecule and that of the fluid particle with which it initially coincided. To obtain these a technique due to Saffman (1960) is used for molecules released well away from the tube wall, and an extension of the same technique is used for molecules released near the tube wall. It is shown how the results can be used to describe the initial stages of dispersion of a cloud of contaminant molecules distributed arbitrarily over the cross-section in any laminar flow, steady or unsteady. Comparisons with some exact results for steady Poiseuille flow in a circular tube confirm that the approximations are formally correct, but show that in certain cases their practical use is limited to very small values of  $T$ , because of the high coefficients of the first two terms neglected in deriving the approximation.

---

### 1. Introduction

Consider a molecule of passive contaminant released at  $t = 0$  in fluid flowing laminarily through a straight tube. Let the speed of the molecule in the direction of the axis at time  $t$  be  $U(t)$ . Now  $U(t)$  is not equal to  $V(t)$ , the longitudinal speed of the fluid particle with which the molecule is instantaneously coincident, because the molecule has a random component of speed  $q(t)$  due to its collisions with other molecules. Thus, following Saffman (1960),

$$U(t) = V(t) + q(t). \quad (1.1)$$

It is important to realize that, like  $q(t)$ ,  $V(t)$  is also a random function of time for, because of the random lateral motions which the molecule undergoes, it coincides, in an unpredictable way, with different fluid particles at different times.

By the definition of a fluid particle the ensemble average of  $q(t)$ , that is the average over all realizations of the molecular motion, is zero for all  $t$ . Thus, denoting such an average by angle brackets,

$$\langle U(t) \rangle = \langle V(t) \rangle. \quad (1.2)$$

The value of  $\langle U(t) \rangle$  depends of course on the initial position of the contaminant molecule, since this fixes the velocity of the fluid particle with which it initially coincides.

To follow this point further consider the specific case of Poiseuille flow in a circular tube of radius  $a$ , and suppose that the molecule is released from  $(x_0, y_0, z_0)$  at  $t = 0$ , where  $y = z = 0$  is the tube axis and  $x$  measures distance along the axis. Then

$$\langle U(0) \rangle = \langle V(0) \rangle = V_0(0) = 2\bar{u}(1 - y_0^2/a^2 - z_0^2/a^2), \quad (1.3)$$

where, throughout this paper,  $V_0(t)$  denotes the velocity at time  $t$  of the fluid particle with which the molecule initially coincided, and  $\bar{u}$  is the discharge velocity. In unsteady laminar flows  $V_0(t)$  depends on time as the notation suggests, but it is not random. Here of course it is constant.

It is not true, even for this simple case of steady flow, that  $\langle V(t) \rangle = V_0(t)$ , although such a result might, at a superficial glance, be expected. For consider a molecule released from a point like  $A$  in figure 1 for times  $t$  satisfying

$$a - (y_0^2 + z_0^2)^{\frac{1}{2}} \gg (\kappa t)^{\frac{1}{2}}, \quad (1.4)$$

where  $\kappa$  is the molecular diffusivity. Provided (1.4) is satisfied the walls play no part in the random motion of the molecule, which is therefore subsequently as likely to be nearer the wall than  $A$  as it is to be further away. This is indicated by the arrows in the figure. But because of the curvature of the velocity profile the molecule suffers a decrease in its longitudinal speed if it moves nearer the wall which is larger than the increase if it moves nearer the axis. Thus, provided that (1.4) holds,  $\langle V(t) \rangle < V_0(t)$ . On the other hand consider a molecule released from a point like  $B$  in figure 1 for times  $t$  satisfying

$$a - (y_0^2 + z_0^2)^{\frac{1}{2}} \lesssim (\kappa t)^{\frac{1}{2}}. \quad (1.5)$$

For such molecules the tube walls seriously inhibit the motion of molecules nearer the wall than  $B$ , so that the longitudinal speed of the molecule increases, on the average. Thus, provided that (1.5) holds,  $\langle V(t) \rangle > V_0(t)$ .

The arguments just given can obviously be applied to many other flows.

Now the dispersion of a cloud of contaminant molecules along the axis of the tube can be described in terms of the statistical properties of the process  $U(t)$ , averaged over the initial positions of the molecules. Such a description is less usual than, though ultimately equivalent to, one based on the diffusion equation. The arguments given above illustrate how a description of the statistics of the motion of an individual molecule can illuminate the physics of the dispersion process. In the remainder of this note further statistical properties of the motion of an individual molecule are obtained for various flows, and this leads to a description of certain features of a dispersing cloud of molecules. The description applies only for times after release which are short compared with that taken for a

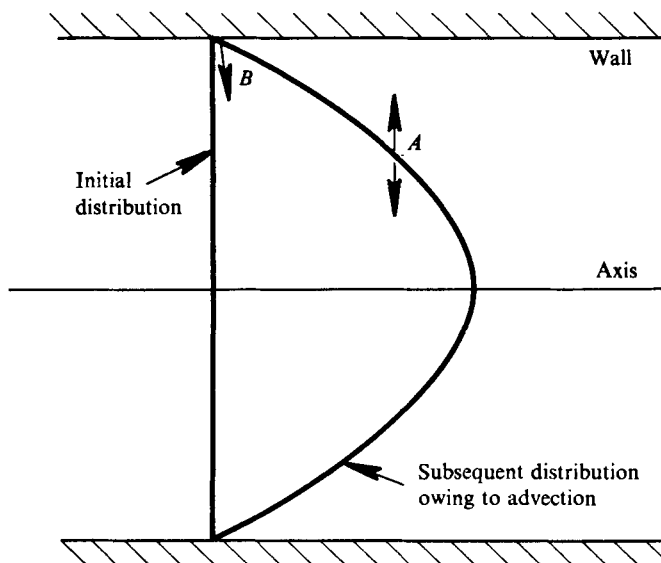


FIGURE 1. Sketch illustrating the way in which the motion of a contaminant molecule is affected by diffusion in Poiseuille flow.

molecule to wander over the tube cross-section; i.e. the analysis is restricted to times  $t$  such that

$$T = \kappa t/a^2 \ll 1. \tag{1.6}$$

Such times are important in many physiological situations (Lighthill 1966) where the total time available for dispersion is limited by the length of the vessel, so that the now classical theory of Taylor (1953) cannot be applied.

The techniques to be used in most of this paper are due to Saffman (1960), who investigated the effect of molecular diffusivity on turbulent diffusion. However it will be shown briefly in the appendix how the results can be obtained by more traditional, though longer and less illuminating methods.

## 2. Dispersion in steady flows, illustrated by Poiseuille flow in a circular tube

Let the axial displacement of a contaminant molecule at time  $t$  after release from  $(x_0, y_0, z_0)$  be  $\dot{X}(t)$ . Then  $\dot{X} = U$ , so that, using (1.2),

$$\langle X(t) \rangle = \int_0^t \langle V(s) \rangle ds. \tag{2.1}$$

For a cloud of contaminant molecules, all released at  $t = 0$  from  $(x_0, y_0, z_0)$ ,  $\langle X(t) \rangle$  is the axial displacement of the centre of mass of the cloud. The spreading of the cloud in the longitudinal direction depends on  $\langle X^2(t) \rangle$ . Now by (1.1),

$$dX^2/dt = 2X(t) U(t) = 2 \int_0^t [V(s) + q(s)][V(t) + q(t)] ds,$$

and so

$$\frac{d}{dt} \langle X^2(t) \rangle = 2 \int_0^t \langle [V(s) + q(s)][V(t) + q(t)] \rangle ds. \tag{2.2}$$

For  $t - s \gg t_c$ , the mean time between molecular collisions, the processes  $V$  and  $q$  are uncorrelated. Since  $t_c \approx 10^{-10}$  s in air under normal conditions (Jeans 1960, p. 49) and is obviously smaller in liquids, in practice (2.2) becomes

$$\frac{d}{dt} \langle X^2(t) \rangle = 2 \int_0^t \langle V(s) V(t) \rangle ds + 2 \int_0^t \langle q(s) q(t) \rangle ds.$$

Now  $\langle q(s) q(t) \rangle$  vanishes when  $t - s \gtrsim t_c$  and it follows that, since in the absence of any bulk motion of the fluid the value of  $d\langle X^2(t) \rangle/dt$  must be  $2\kappa$ , where  $\kappa$  is the molecular diffusivity, then

$$\frac{d}{dt} \langle X^2(t) \rangle = 2 \int_0^t \langle V(s) V(t) \rangle ds + 2\kappa, \quad (2.3)$$

for  $t \gg t_c$ . Further details of the argument leading to (2.3) can be found in Saffman (1960), to whom the result is due.

#### The determination of $\langle V(s) \rangle$ and $\langle V(s) V(t) \rangle$

Now  $\langle V(s) \rangle$  is the average of  $u(y, z)$ , the steady axial component of the fluid velocity, weighted with the probability distribution of the position of the molecule. That is (Saffman 1960),

$$\langle V(s) \rangle = \iiint u(y, z) C(x, y, z, s | x_0, y_0, z_0) dx dy dz, \quad (2.4)$$

where  $C(x, y, z, s | x_0, y_0, z_0) dx dy dz$  is the probability that at time  $s$  after release from  $(x_0, y_0, z_0)$  a marked molecule is in a volume of size  $dx dy dz$  surrounding  $(x, y, z)$ . Thus  $C$  is the (suitably normalized) distribution of concentration associated with initial release from  $(x_0, y_0, z_0)$ .

Consider first a case when  $\eta_0$ , the distance of the initial position of the molecule from the tube wall, and  $s$  satisfy

$$\eta_0 \gg (\kappa s)^{\frac{1}{2}}. \quad (2.5)$$

In a circular tube of radius  $a$ ,  $\eta_0 = a - (y_0^2 + z_0^2)^{\frac{1}{2}}$ , so that, with  $s$  replacing  $t$ , (2.5) is the same as (1.4). When (2.5) holds, the tube walls play no part in the determination of  $C$ , so that for small values of  $S = \kappa s/a^2$  the form of  $C$  is (Saffman 1960)

$$C(x, y, z, s | x_0, y_0, z_0) = \frac{1}{8(\pi\kappa s)^{\frac{3}{2}}} \exp \left[ - \left\{ \frac{(x - x_0 - u(y_0, z_0) s)^2 + (y - y_0)^2 + (z - z_0)^2}{4\kappa s} \right\} \right] [1 + O(S)]. \quad (2.6)$$

Thus the cloud spreads isotropically about the fluid particle initially at the position of release entirely as the result of molecular diffusion. The result for  $C$  in (2.6) is discussed further in Chatwin (1976), where it is shown how the higher-order terms in (2.6) can be related to the deviations of the fluid velocity field from uniformity in the neighbourhood of  $(x_0, y_0, z_0)$ . On expanding  $u(y, z)$  in a Taylor series about  $(x_0, y_0, z_0)$  it now follows from (2.4) and (2.6) that

$$\langle V(s) \rangle = V_0(s) + \kappa s \nabla^2 u(y_0, z_0) [1 + O(S)], \quad (2.7)$$

where, for the present case of steady flow,

$$V_0(s) = V_0(0) = u(y_0, z_0). \quad (2.8)$$

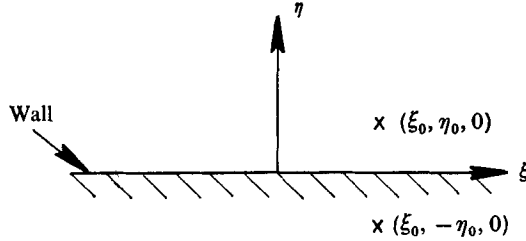


FIGURE 2. Definition of axes when the initial position of the molecule is near the wall.

Note that the difference between  $\langle V(s) \rangle$  and  $V_0(s)$  is proportional to  $\nabla^2 u$ , which measures the curvature of the velocity profile. Also  $\nabla^2 u$  is negative in unidirectional steady flows in straight tubes. Thus (2.7), given by Saffman (1960), agrees with the argument of § 1.

Saffman was concerned with unbounded flows for which (2.7) holds for all initial positions. However in flows in a tube, the concern of this note, it is necessary to consider initial positions whose distance  $\eta_0$  from the tube walls does not satisfy (2.5), but rather

$$\eta_0 \lesssim (\kappa s)^{\frac{1}{2}}. \quad (2.9)$$

When (2.9) holds, the form of  $C$  given by (2.6) is not adequate, since it does not satisfy the condition  $\mathbf{n} \cdot \nabla C = 0$  at the wall.† However it is obvious that to a first approximation the tube wall can be considered plane, so that  $C$  can be obtained by adding to (2.6) the value of  $C$  for release from the image of  $(x_0, y_0, z_0)$  in the tube wall. For simplicity it is convenient to change axes to those shown in figure 2, where  $\xi = x$ ,  $\eta$  measures distance from the tube wall, and  $\zeta$  measures distance around the tube wall. Then the initial position of the molecule can be taken as  $(\xi_0, \eta_0, 0)$  with image at  $(\xi_0, -\eta_0, 0)$ . Thus the form of  $C$  is, to highest order,

$$C(\xi, \eta, \zeta, s | \xi_0, \eta_0, 0) \approx \frac{1}{8(\pi \kappa s)^{\frac{3}{2}}} \exp \left[ - \left\{ \frac{(\xi - \xi_0 - u(\eta_0, 0) s)^2 + \zeta^2}{4 \kappa s} \right\} \right] \\ \times \left\{ \exp \left[ - \frac{(\eta - \eta_0)^2}{4 \kappa s} \right] + \exp \left[ - \frac{(\eta + \eta_0)^2}{4 \kappa s} \right] \right\}, \quad (2.10)$$

and (2.10) holds only in  $\eta \geq 0$ . Use of (2.4) now gives

$$\langle V(s) \rangle = V_0(s) + 2 \left( \frac{\kappa s}{\pi} \right)^{\frac{1}{2}} \left( \frac{\partial u}{\partial \eta} \right)_{\text{wall}} \left[ \exp \left\{ - \frac{\eta_0^2}{4 \kappa s} \right\} - \frac{\eta_0}{2} \left( \frac{\pi}{\kappa s} \right)^{\frac{1}{2}} \left\{ 1 - \operatorname{erf} \left( \frac{\eta_0}{2 \sqrt{\kappa s}} \right) \right\} \right] \\ \times [1 + O(S^{\frac{1}{2}})], \quad (2.11)$$

where  $V_0(s)$  is given by (2.8). The term  $O(S^{\frac{1}{2}})$  in (2.11) depends in detail on the geometry of the tube walls and it has not been found possible to derive a general expression for it, valid in all geometries. The function of  $\eta_0/2(\kappa s)^{\frac{1}{2}}$  in square brackets is everywhere positive, so that, since  $(\partial u/\partial \eta)_{\text{wall}} > 0$ , (2.11) predicts that  $\langle V(s) \rangle > V_0(s)$  whenever (2.9) holds, again in agreement with the argument in § 1.

† It would be of interest to try to develop the methods of this paper to cover the more general boundary condition  $\alpha \mathbf{n} \cdot \nabla C + \beta C = 0$  at the tube wall but it is not clear whether this would be a practical proposition, or even tractable.

The value of  $\langle V(s) V(t) \rangle$  is a function only of  $t - s$  in those cases where  $V(s)$  is a stationary random function of  $s$  (Taylor 1921; Saffman 1960). Here, however,  $V(s)$  does not satisfy this condition just after release because it is influenced by the known initial position. Thus  $\langle V(s) V(t) \rangle$  depends on both  $s$  and  $t$  and has to be determined using the joint probability distribution of the positions of the molecule at  $s$  and  $t$ . This joint probability distribution is the probability that the molecule is in a neighbourhood of one point, say  $\mathbf{x}'$ , at time  $s$  and in the neighbourhood of a second point, say  $\mathbf{x}$ , at time  $t$ . Thus the joint probability distribution is

$$C(\mathbf{x}', s | \mathbf{x}_0) C(\mathbf{x}, t - s | \mathbf{x}'), \quad (2.12)$$

where  $C$  is defined in (2.6) or (2.10) as appropriate. Then

$$\langle V(s) V(t) \rangle = \iint u(\mathbf{x}') u(\mathbf{x}) C(\mathbf{x}', s | \mathbf{x}_0) C(\mathbf{x}, t - s | \mathbf{x}') d^3\mathbf{x} d^3\mathbf{x}'. \quad (2.13)$$

In a case when the initial position of the molecule is far from the walls, so that (2.5) and (2.6) hold, it follows from (2.13) that

$$\langle V(s) V(t) \rangle = u^2(y_0, z_0) + \kappa s \nabla^2 u^2(y_0, z_0) + \kappa(t - s) u(y_0, z_0) \nabla^2 u(y_0, z_0) [1 + O(T)]. \quad (2.14)$$

On the other hand, when the molecule is initially near the wall, so that (2.9) and (2.10) hold, it is possible to show after some algebra that  $\langle V(s) V(t) \rangle$  differs from (2.14) only in the error term, which is now  $O(T^{\frac{1}{2}})$ .

#### *Properties of a dispersing cloud*

So far in this paper the discussion has been confined to molecules released from a single initial position  $(x_0, y_0, z_0)$ . Now consider the dispersion of a cloud of molecules initially distributed over the cross-section  $x = 0$  (without loss of generality) with density per unit area  $F(y_0, z_0)$ , so that provided  $F$  is normalized such that

$$\iint F(y_0, z_0) dy_0 dz_0 = 1, \quad (2.15)$$

$F(y_0, z_0) \delta y_0 \delta z_0$  is the fraction of the molecules whose initial position lies in an area  $\delta y_0 \delta z_0$  containing  $(y_0, z_0)$ . (The dispersion of a group of molecules not initially all at  $x = 0$  can be obtained from the following results by superposition.) Let  $x_g(t)$  and  $\sigma^2(t)$  be the axial displacement of the centre of mass and the longitudinal variance at time  $t$  after release; evidently  $x_g(0) = \sigma^2(0) = 0$ .

Assuming that the total number of marked molecules is large enough for the averages over the cloud to be practically indistinguishable from the ensemble averages,  $x_g(t)$  is the average of  $\langle X(t) \rangle$  weighted with  $F(y_0, z_0)$  over all  $(y_0, z_0)$ , where  $\langle X(t) \rangle$  satisfies (2.1). Thus, using the expression (2.7) for  $\eta_0$  satisfying (2.5), and the expression (2.11) for  $\eta_0$  satisfying (2.9) it follows that

$$\begin{aligned} dx_g/dt \approx & \iint u(y_0, z_0) F(y_0, z_0) dy_0 dz_0 + \kappa t \iint \nabla^2 u(y_0, z_0) F(y_0, z_0) dy_0 dz_0 \\ & + 2 \left( \frac{\kappa t}{\pi} \right)^{\frac{1}{2}} \left( \oint \frac{\partial u}{\partial \eta} F dl \right) \int_0^\infty \left[ \exp \left( -\frac{\eta_0^2}{4\kappa s} \right) - \frac{\pi^{\frac{1}{2}} \eta_0}{2(\kappa s)^{\frac{1}{2}}} \left\{ 1 - \operatorname{erf} \left( \frac{\eta_0}{2(\kappa s)^{\frac{1}{2}}} \right) \right\} \right] d\eta_0, \end{aligned}$$

where the surface integrals are over the whole cross-section and the line integral is round the perimeter of the cross-section. The first term in this expression comes

from the first terms in (2.7) and (2.11), while the second and third terms come from the second terms in (2.7) and (2.11) respectively. On performing the integral with respect to  $\eta_0$  in the third term and applying Gauss's theorem to the line integral, it follows that

$$dx_g/dt \approx \iint u(y_0, z_0) [F(y_0, z_0) + \kappa t \nabla^2 F(y_0, z_0)] dy_0 dz_0. \quad (2.16)$$

(Note that the second term in the previous expression for  $dx_g/dt$  is cancelled exactly by one of the terms arising from the application of Gauss's theorem.)

Some implications of (2.16) are of interest. First, if  $F(y_0, z_0)$  is uniform, then  $dx_g/dt \approx \bar{u}$ . In fact it can be shown that this result holds exactly for all time as might be expected, for when  $F(y_0, z_0)$  is uniform the molecules of contaminant are distributed uniformly over the cross-section, so that, since they are passive, their mean longitudinal velocity, as a group, is the mean longitudinal velocity of all fluid molecules, i.e. the discharge velocity  $\bar{u}$ . This means that the tendency of contaminant molecules in the bulk of the flow to lag behind the fluid particles is exactly balanced, when  $F$  is uniform, by the tendency of molecules near the wall to move faster than the fluid particles there. When  $F$  is not uniform, the two opposing effects do not normally cancel. In particular, if  $\nabla^2 F > 0$  everywhere, as occurs when  $F$  increases monotonically (nonlinearly) with distance from the centre of the tube to the wall, (2.16) confirms that the centre of mass of the cloud moves faster, because of the greater relative importance of the molecules near the wall, than the centre of mass of the cloud of fluid particles with which the molecules initially coincided. A converse result holds when  $\nabla^2 F < 0$  everywhere.

Passing now to the longitudinal spread of the cloud, an analysis similar to that leading to (2.16), but based on (2.3) rather than (2.1) and (2.14) rather than (2.7) and (2.11), gives after integrating with respect to  $\eta_0$

$$\begin{aligned} \frac{d}{dt} \langle X^2(t) \rangle \approx & 2\kappa + 2t \iint u^2(y_0, z_0) F(y_0, z_0) dy_0 dz_0 \\ & + \kappa t^2 \iint [\nabla^2 u^2(y_0, z_0) + u(y_0, z_0) \nabla^2 u(y_0, z_0)] F(y_0, z_0) dy_0 dz_0. \end{aligned} \quad (2.17)$$

To the order of approximation in (2.17) (where terms proportional to  $t^{\frac{3}{2}}$  have not been included) no distinctive contribution comes from the region near the wall, essentially because  $\partial u^2/\partial \eta$  is zero at the wall (whereas  $\partial u/\partial \eta$ , which causes the distinctive contribution in the expression for  $dx_g/dt$ , is not zero). Now  $\sigma^2(t)$ , the variance of the cloud in the axial direction, satisfies

$$\sigma^2 = \langle X^2 \rangle - \{\langle X \rangle\}^2,$$

so that, integrating (2.16) and (2.17) with respect to  $t$ ,

$$\begin{aligned} \sigma^2(t) \approx & 2\kappa t + t^2 \left[ \iint u^2 F dy_0 dz_0 - \left( \iint u F dy_0 dz_0 \right)^2 \right] \\ & + \frac{1}{3} \kappa t^3 \left[ \iint [\nabla^2 u^2 + u \nabla^2 u] F dy_0 dz_0 - 3 \left( \iint u F dy_0 dz_0 \right) \left( \iint u \nabla^2 F dy_0 dz_0 \right) \right]. \end{aligned} \quad (2.18)$$

The first term in (2.18) is the effect of direct longitudinal molecular diffusion, the second term is the variance of the fluid particles initially coincident with the molecules and the third term is the highest-order effect of the difference between fluid-particle and molecular motion.

*Some details for the case of Poiseuille flow in a circular tube*

To illustrate the results above return to the case of Poiseuille flow in a circular cylinder of radius  $a$ , for which the velocity profile is given in (1.3), viz.

$$u(y_0, z_0) = 2\bar{u}(1 - y_0^2/a^2 - z_0^2/a^2). \quad (2.19)$$

Although (2.19) is simple, it is realizable in practice and representative of the general situation. In order to illustrate the theory it is necessary to consider special forms for  $F(y_0, z_0)$ , the initial distribution of contaminant molecules over  $x = 0$ , so results are presented for three cases  $A$ ,  $B$  and  $C$  in which  $F$  is given by

$$F(y_0, z_0) = \begin{cases} 1/\pi a^2 & \text{(case A),} \\ (2/\pi a^4)(y_0^2 + z_0^2) & \text{(case B),} \\ (2/\pi a^4)(a^2 - y_0^2 - z_0^2) & \text{(case C).} \end{cases} \quad (2.20)$$

$$(2.21)$$

$$(2.22)$$

These represent situations where the initial distribution is uniform (case  $A$ ), increasing monotonically from the axis to the wall (case  $B$ ) and decreasing monotonically from the axis to the wall (case  $C$ ). Evaluation of the integrals in (2.16) and (2.18) gives the following results, where

$$\mu = x_0(\kappa/\bar{u}a^2), \quad \Sigma^2 = (\sigma^2 - 2\kappa t)(\kappa/\bar{u}a^2)^2. \quad (2.23)$$

In case  $A$

$$\mu \approx T, \quad \Sigma^2 \approx T^2\{\frac{1}{3} - \frac{8}{3}T + \dots\}; \quad (2.24)$$

in case  $B$

$$\mu \approx T\{\frac{2}{3} + 4T + \dots\}, \quad \Sigma^2 \approx T^2\{\frac{2}{9} - \frac{32}{9}T + \dots\}; \quad (2.25)$$

in case  $C$

$$\mu \approx T\{\frac{4}{3} - 4T + \dots\}, \quad \Sigma^2 \approx T^2\{\frac{2}{9} + \frac{32}{9}T + \dots\}. \quad (2.26)$$

For these three cases the values of  $\mu$  and  $\Sigma^2$  can be determined exactly after some lengthy algebra which is summarized in the appendix to this paper. The exact results confirm the formal correctness of the approximations (2.24)–(2.26), but show also that the coefficients of the terms in  $T^{\frac{3}{2}}$  and  $T^2$  [the first two terms ignored in the curly brackets in (2.24)–(2.26)] are numerically large, especially in cases  $B$  and  $C$ , and especially for  $\Sigma^2$ .

As far as  $\mu$  is concerned the approximation in case  $A$  is exact for all values of  $T$ , whereas, as figure 3 shows, the error in case  $B$  (and therefore in case  $C$ ) caused by using the approximation progressively increases with time, reaching 3.3% for  $T = 0.02$  and 11.3% for  $T = 0.05$ . There is an error in all three cases when the approximation is used for  $\Sigma^2$ . For case  $A$ , when the initial distribution is uniform over the pipe cross-section, the error increases from 2.6% at  $T = 0.02$  to 20.6% at  $T = 0.05$ . However in case  $B$  (and in case  $C$ ) significant errors occur for smaller values of  $T$  than in case  $A$ , so that there is an error of 8.3% at  $T = 0.01$  and an error of 21.6% at  $T = 0.02$ . Furthermore in case  $B$  (and  $C$ ) the values in figure 4 show that these errors are so large that, as far as calculating  $\Sigma^2$  is concerned, the



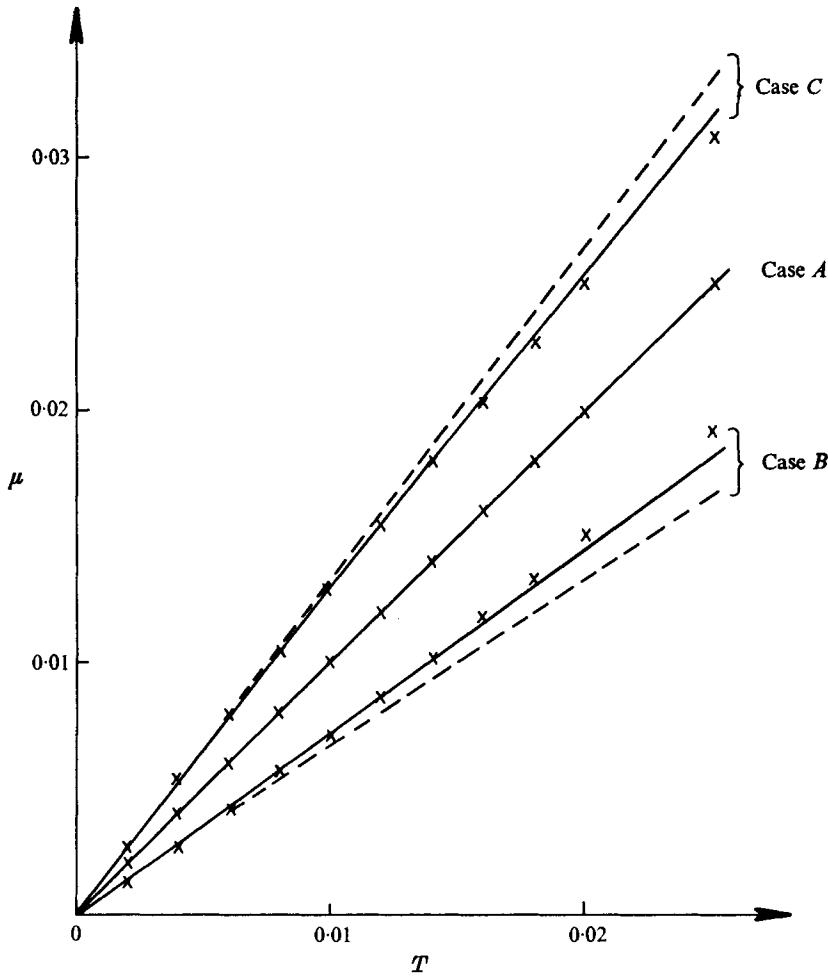


FIGURE 3. Graphs of  $\mu$  for cases *A*, *B* and *C*. —, exact values; ---, values for fluid particles; x, values given by approximations (2.24)–(2.26). Note that in case *A* all three graphs coincide.

difference between fluid particles and molecules is important only if the terms of order  $T^{\frac{3}{2}}$  and  $T^2$  can be added explicitly to the expressions in curly brackets for  $\Sigma^2$  in (2.25) and (2.26). This is not a practical proposition using the methods of this paper, for although it is perhaps possible to derive extra terms in the expressions (2.6) for  $C$  in unbounded space (in the manner outlined by Chatwin, 1976), it would be extremely difficult (and prohibitively long) to derive extra terms in the expression (2.10) for  $C$  near the wall. Note also that the approximation to  $\Sigma^2$  in case *B* is an underestimate whereas that in case *C* is an overestimate, so that the relatively small errors in the approximation to  $\Sigma^2$  in case *A* result from these large errors of opposite sign tending to cancel. These somewhat disappointing conclusions about the practical value of the approximations to  $\Sigma^2$  are not surprising in view of the well-known singular behaviour of solutions of parabolic equations for  $t = 0+$ .

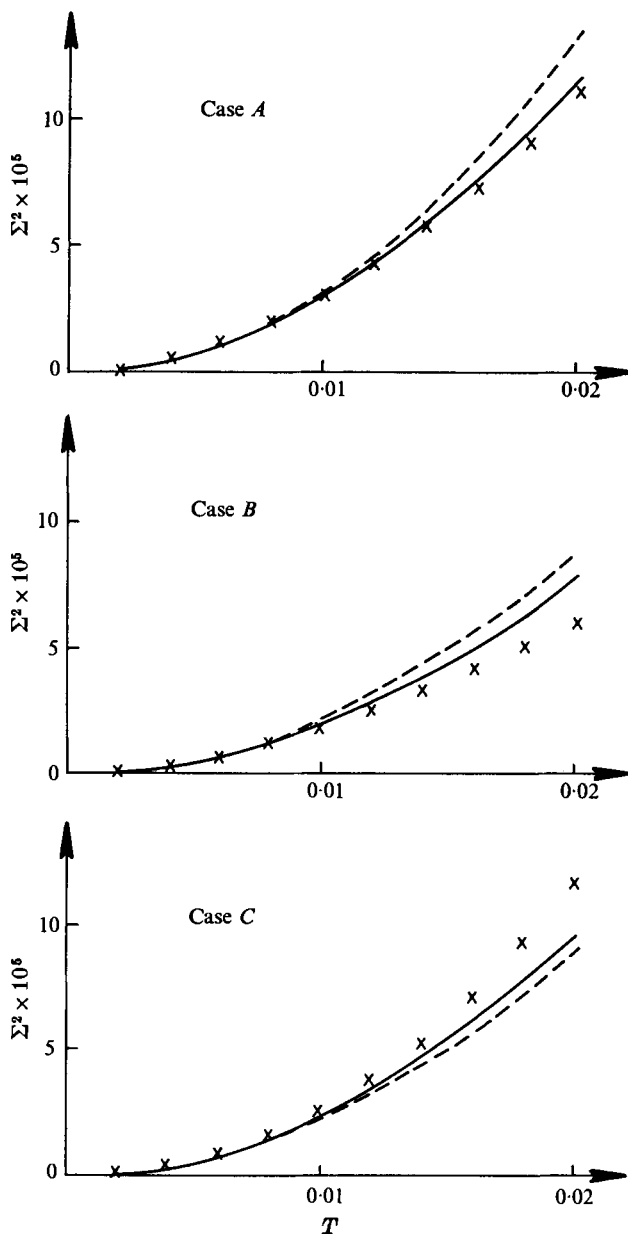


FIGURE 4. Graphs of  $\Sigma^2$  for cases *A*, *B* and *C*. —, exact values; ---, values for fluid particles; x, values given by approximations (2.24)–(2.26).

By means of the principle of superposition, further solutions can be built up from those for any two of cases *A*, *B* and *C*. For example, denoting cases *B* and *C* by the appropriate subscripts, the values of  $\mu$  and  $\Sigma^2$  for an initial distribution  $F(y_0, z_0) = \alpha F_B + (1 - \alpha) F_C$  (where  $0 \leq \alpha \leq 1$  for  $F$  to be everywhere positive) satisfy

$$\left. \begin{aligned} \mu &= \alpha \mu_B + (1 - \alpha) \mu_C, \\ \Sigma^2 + \mu^2 &= \alpha (\Sigma_B^2 + \mu_B^2) + (1 - \alpha) (\Sigma_C^2 + \mu_C^2). \end{aligned} \right\} \quad (2.27)$$

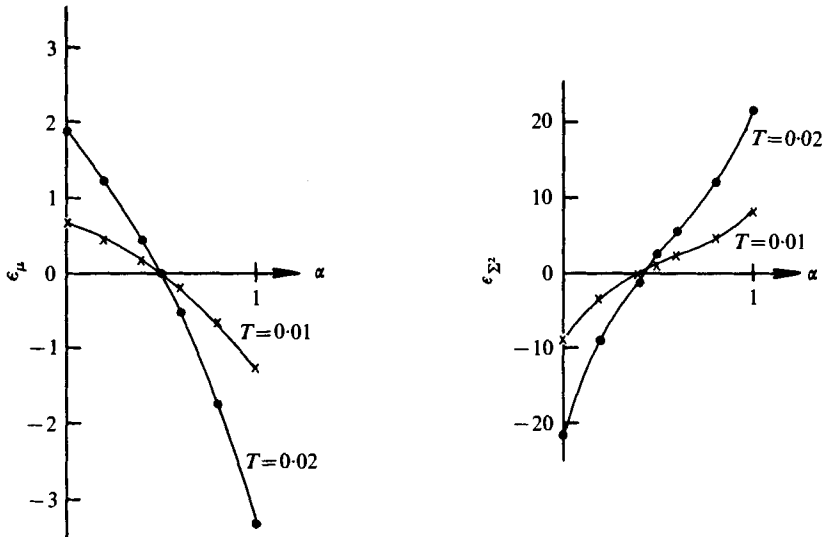


FIGURE 5. Errors in using the approximations for various values of  $\alpha$ .  $\epsilon_\mu = 100 (1 - \mu_{\text{approx}}/\mu_{\text{exact}})$ ,  $\epsilon_{\Sigma^2} = 100 (1 - \Sigma^2_{\text{approx}}/\Sigma^2_{\text{exact}})$ . The appropriate values are obtained from (2.27).

(Note that it is  $\Sigma^2 + \mu^2$ , not  $\Sigma^2$ , which is a linear function of  $F$ .) In figure 5 the percentage errors caused by using the approximations developed in this paper are plotted for two values of  $T$  and various values of  $\alpha$ . It will be noted that the errors are greatest when  $\alpha = 1$  (case *B*) and when  $\alpha = 0$  (case *C*), and smallest near  $\alpha = 0.5$  (case *A*). Detailed calculations show that the first term neglected in the approximation for  $\Sigma^2$  has a zero coefficient when  $\alpha = 0.395$ , and this is consistent with the graph.

The approximations to both  $\mu$  and  $\Sigma^2$  are in all cases accurate to within 8% for  $T \lesssim 0.01$ . Such low values of  $T$  are important in applications; for example blood passes right through the human aorta in times such that  $T \approx 5 \times 10^{-5}$ . Nevertheless the main interest of the methods and results of this paper may be theoretical since for such low values of  $T$  the differences between fluid particle and contaminant molecule motion predicted by the approximations are rather small.

### 3. An extension to unsteady unidirectional flows

Although blood flow in the aorta has been cited above as an example where very small values of  $T$  are important, the flow is unsteady, so that the methods and results of §2 cannot be applied. In this section it will be shown how the previous arguments can be extended to cover unsteady unidirectional laminar flows, although no account is taken of secondary flows.

For simplicity consider the specific case of flow through a straight tube with axial velocity  $u(y, z) \cos \omega t$ , where  $y$  and  $z$  are co-ordinates in the cross-section, as in the earlier sections of this paper. More general flows can be dealt with by natural extensions of the techniques to be described. Now many of the results in the previous sections hold for unsteady flows without modification and, in particular,

expressions (2.1) and (2.3) remain true; in these  $\langle X(t) \rangle$  and  $\langle X^2(t) \rangle$  are expressed in terms of  $\langle V(s) \rangle$  and  $\langle V(s) V(t) \rangle$ . By definition  $V(s)$  is the velocity (at time  $s$ ) of the fluid particle with which the contaminant molecule coincides at time  $s$ . So in the unsteady laminar flow being considered (but evidently *not* in turbulent flow)  $V(s) = W(s) \cos \omega s$ , where  $W(s)$  is the value of  $u(y, z)$  at the instantaneous position of the molecule. Thus

$$\langle V(s) \rangle = \langle W(s) \rangle \cos \omega s \quad \text{and} \quad \langle V(s) V(t) \rangle = \langle W(s) W(t) \rangle \cos \omega s \cos \omega t,$$

where  $\langle W(s) \rangle$  and  $\langle W(s) W(t) \rangle$  can be determined from  $C$  and  $u(y, z)$  exactly as described in §2. To the order considered in this paper the form of  $C$  in unsteady laminar flows differs from that in steady flows only because the axial displacement of the fluid particle with which the contaminant molecule initially coincided is  $u(y_0, z_0) \sin(\omega s)/\omega$  rather than  $u(y_0, z_0) s$ . But because of the homogeneity of the flow in the axial direction the values of  $\langle W(s) \rangle$  and  $\langle W(s) W(t) \rangle$  are unaffected by this change, so that, in terms of  $u(y, z)$ , they are given by the expressions derived for  $\langle V(s) \rangle$  and  $\langle V(s) V(t) \rangle$  in §2. Hence, in the flow considered here, the results (2.16) and (2.17) is replaced by

$$dx_g/dt \approx \cos \omega t \iint u(y_0, z_0) [F(y_0, z_0) + \kappa t \nabla^2 F(y_0, z_0)] dy_0 dz_0 \quad (3.1)$$

and

$$\begin{aligned} \frac{d}{dt} \langle X^2(t) \rangle \approx & 2\kappa + \frac{\sin 2\omega t}{\omega} \iint u^2(y_0, z_0) F(y_0, z_0) dy_0 dz_0 \\ & + \frac{\kappa t}{\omega} \sin 2\omega t \iint \nabla^2 u^2(y_0, z_0) F(y_0, z_0) dy_0 dz_0 \\ & + \frac{2\kappa}{\omega^2} \cos \omega t (1 - \cos \omega t) \iint [u(y_0, z_0) \nabla^2 u(y_0, z_0) \\ & - \nabla^2 u^2(y_0, z_0)] F(y_0, z_0) dy_0 dz_0. \end{aligned} \quad (3.2)$$

From these results, those analogous to (2.24)–(2.26) can be obtained by integration. In particular, when the initial distribution of contaminant is uniform over the cross-section, so that  $F$  is given by (2.20), and when  $u(y_0, z_0)$  satisfies (2.19), then (2.24) is replaced by

$$\left. \begin{aligned} \mu & \approx T(\sin(\omega t)/\omega t), \\ \Sigma^2 & \approx T^2 \left\{ \frac{1}{3} \left( \frac{\sin \omega t}{\omega t} \right)^2 - T \left( \frac{4 \sin \omega t - 2\omega t - \sin 2\omega t}{\omega^3 t^3} \right) + \dots \right\}, \end{aligned} \right\} \quad (3.3)$$

and similar, but more complicated, results hold when  $F$  is given by (2.21) and (2.22). In each case it can be verified that the results approach the steady results as  $\omega t \rightarrow 0$  (for fixed  $t$ ), but results like (3.3) hold for all values of  $\omega t$  provided, as in §2, that  $T \ll 1$ .

### Appendix. The exact values of the moments

This appendix outlines the way in which the exact values of  $\mu$  and  $\Sigma^2$  are obtained for the cases considered in detail in §2. The tube has a circular cross-section and the axial velocity satisfies (2.19). Thus  $C(x, y, z, T)$  satisfies

$$\frac{\partial C}{\partial T} + \frac{2\bar{u}a^2}{\kappa} \left(1 - \frac{r^2}{a^2}\right) \frac{\partial C}{\partial x} = a^2 \nabla^2 C, \quad (\text{A } 1)$$

where  $r^2 = y^2 + z^2$ , together with the boundary condition

$$\partial C / \partial r = 0 \quad \text{at} \quad r = a. \quad (\text{A } 2)$$

In addition, there is an initial condition which, for present purposes, can be taken as

$$C(x, y, z, 0) = \delta(x) F(y, z), \quad (\text{A } 3)$$

where  $F$  satisfies the normalization condition (2.15). The values of  $\mu$  and  $\Sigma^2$  when  $F$  is uniform and satisfies (2.20) (case *A*) are determined by Chatwin (1970) with the results

$$\mu = T, \quad (\text{A } 4)$$

$$\Sigma^2 = \left\{ \frac{1}{24} T - \frac{1}{360} + 128 \sum_{n=1}^{\infty} \frac{\exp(-\alpha_n^2 T)}{\alpha_n^6} \right\}, \quad (\text{A } 5)$$

where  $\alpha_n$  is the  $n$ th non-zero root of  $J_1$ . From (A 5) it is not easy to obtain an approximation to  $\Sigma^2$  for  $T \ll 1$ , the subject of this paper. However, the method used to derive (A 5) is the Laplace transformation from which such an approximation can be obtained easily, with the result

$$\Sigma^2 \approx T^2 \left\{ \frac{1}{3} - \frac{8}{3} T + \frac{1024}{105\pi^2} T^{\frac{3}{2}} - 4T^2 + \dots \right\}. \quad (\text{A } 6)$$

The method of obtaining (A 6) is illustrated below. For the moment note that, as stated in §2, (A 6) is consistent with the approximation (2.23).

Consider now case *B*, when  $F$  satisfies (2.21). Evidently  $C$  is axially symmetric, so that  $C = C(x, r, T)$ . Define

$$R = r/a, \quad (\text{A } 7)$$

and then  $C_n(R, T)$  and  $\hat{C}_n(R, p)$  for each integer  $n \geq 0$  by

$$C_n(R, T) = \left( \frac{\kappa}{\bar{u}a^2} \right)^{n+1} \int_{-\infty}^{\infty} x^n C dx, \quad \hat{C}_n(R, p) = \int_0^{\infty} C_n e^{-pT} dT. \quad (\text{A } 8)$$

Equations for the  $C_n$  are obtained from (A 1) in the manner described by Aris (1956), and those for the  $\hat{C}_n$  by taking the Laplace transformation defined in (A 8). When  $F$  satisfies (2.21) the following results are obtained for  $n = 0, 1$  and  $2$ :

$$\frac{d^2 \hat{C}_0}{dR^2} + \frac{1}{R} \frac{d\hat{C}_0}{dR} - p\hat{C}_0 = -\frac{2R^2}{\pi a^2} \left( \frac{\kappa}{\bar{u}a^2} \right); \quad (\text{A } 9)$$

$$\frac{d^2 \hat{C}_1}{dR^2} + \frac{1}{R} \frac{d\hat{C}_1}{dR} - p\hat{C}_1 = -2(1 - R^2) \hat{C}_0; \quad (\text{A } 10)$$

$$\frac{d^2 \hat{C}_2}{dR^2} + \frac{1}{R} \frac{d\hat{C}_2}{dR} - p\hat{C}_2 = -4(1 - R^2) \hat{C}_1 - 2 \left( \frac{\kappa}{\bar{u}a^2} \right)^2 \hat{C}_0. \quad (\text{A } 11)$$

Also from (A 2) it follows that

$$d\hat{C}_n/dR = 0 \quad \text{at} \quad R = 1. \quad (\text{A } 12)$$

The solution of (A 9) which satisfies (A 12) is

$$\hat{C}_0 = \frac{2}{\pi a^2 p^2} \left( \frac{\kappa}{\bar{u} a^2} \right) \left\{ 4 + s^2 - \frac{2I_0(s)}{I_1(p^{\frac{1}{2}})} p^{\frac{1}{2}} \right\}, \quad (\text{A } 13)$$

where  $s = R p^{\frac{1}{2}}$  (A 14)

and  $I_0$  and  $I_1$  are modified Bessel functions. Now  $x_g$  satisfies, using the normalization condition (2.15),

$$x_g = 2\pi \iint C x r \, dx \, dr,$$

so that, from (2.23) and (A 8),

$$\mu = 2\pi a^2 \left( \frac{\bar{u} a^2}{\kappa} \right) \int_0^1 R C_1 \, dR, \quad (\text{A } 15)$$

and on multiplying (A 10) by  $R$ , integrating from 0 to 1, and using (A 12) and the Laplace transformation of (A 15), it follows that

$$\hat{\mu} = \frac{4\pi a^2}{p} \left( \frac{\bar{u} a^2}{\kappa} \right) \int_0^1 R(1-R^2) \hat{C}_0 \, dR. \quad (\text{A } 16)$$

Thus, on substituting (A 13) into (A 16) and integrating,

$$\hat{\mu} = \frac{64}{p^4} + \frac{8}{p^3} + \frac{2}{3p^2} - \frac{32I_0(p^{\frac{1}{2}})}{p^{\frac{1}{2}}I_1(p^{\frac{1}{2}})}. \quad (\text{A } 17)$$

Now on expanding  $I_0(p^{\frac{1}{2}})/I_1(p^{\frac{1}{2}})$  about  $p = 0$  it turns out that  $\hat{\mu} \approx 1/p^2 - 1/48p$  near  $p = 0$ . Also, the zeros of  $I_1(p^{\frac{1}{2}})$  are simple and on the negative real axis with  $p = -\alpha_n^2$ , where  $\alpha_n$  is the  $n$ th non-zero root of  $J_1$ . Thus, inverting (A 17),

$$\mu = \left\{ T - \frac{1}{48} + 64 \sum_{n=1}^{\infty} \frac{\exp(-\alpha_n^2 T)}{\alpha_n^6} \right\}. \quad (\text{A } 18)$$

But as with (A 5) this form is not useful for determining  $\mu$  for  $T \ll 1$ . However for large  $p^{\frac{1}{2}}$ ,  $I_0(p^{\frac{1}{2}})/I_1(p^{\frac{1}{2}}) \approx 1 + (1/2p^{\frac{1}{2}}) + \dots$ , so that, inverting (A 17) directly,

$$\mu \approx T \left\{ \frac{2}{3} + 4T - \frac{256}{15\pi^{\frac{1}{2}}} T^{\frac{3}{2}} + 8T^2 + \dots \right\}. \quad (\text{A } 19)$$

As stated in §2, this verifies the correctness of the approximation (2.25) derived in the paper.

Turning now to  $\sigma^2$ , note that

$$\sigma^2 = 2\pi \iint x^2 C r \, dr \, dx - x_g^2,$$

so that, from (2.23) and (A 8),

$$\Theta \equiv \Sigma^2 + \mu^2 = 2\pi a^2 \left( \frac{\bar{u} a^2}{\kappa} \right) \int_0^1 R C_2 \, dR - 2T \left( \frac{\kappa}{\bar{u} a} \right)^2, \quad (\text{A } 20)$$

so that on multiplying (A 11) by  $R$ , integrating from 0 to 1, and using (A 12) and the Laplace transformation of (A 20), it follows that

$$\hat{\Theta} = \frac{4\pi a^3}{p} \left( \frac{\kappa}{\bar{u}a} \right) \int_0^1 R \hat{C}_0 dR + \frac{8\pi a^3}{p} \left( \frac{\bar{u}a}{\kappa} \right) \int_0^1 R(1-R^2) \hat{C}_1 dR - \frac{2}{p^2} \left( \frac{\kappa}{\bar{u}a} \right)^2. \quad (\text{A } 21)$$

By multiplying (A 9) by  $R$  and integrating from 0 to 1 it follows that

$$\int_0^1 R \hat{C}_0 dR = \frac{1}{2\pi p a^3} \left( \frac{\kappa}{\bar{u}a} \right). \quad (\text{A } 22)$$

A similar procedure can be used to evaluate the second term in (A 21), and although the algebra is long, this is quicker than solving (A 10) for  $\hat{C}_1$  directly. Now (A 10) can be written

$$\frac{d^2 \hat{C}_1}{ds^2} + \frac{1}{s} \frac{d \hat{C}_1}{ds} - \hat{C}_1 = f(s), \quad (\text{A } 23)$$

where  $f(s)$  is given explicitly by substituting (A 13) into (A 10). The required second term of (A 21) is

$$\int_0^1 R(1-R^2) \hat{C}_1 dR = \frac{1}{p} \int_0^{p^\dagger} s \hat{C}_1 ds - \frac{1}{p^2} \int_0^{p^\dagger} s^3 \hat{C}_1 ds. \quad (\text{A } 24)$$

From (A 23) it follows in the manner used several times in this appendix that

$$\int_0^{p^\dagger} s \hat{C}_1 ds = - \int_0^{p^\dagger} s f(s) ds, \quad (\text{A } 25)$$

and this can be evaluated explicitly. Also, multiplying (A 23) by  $s^3$  and integrating gives

$$\int_0^{p^\dagger} s^3 \hat{C}_1 ds = -4 \int_0^{p^\dagger} s f ds - \int_0^{p^\dagger} s^2 f ds - 2p \hat{C}_1(p^\dagger), \quad (\text{A } 26)$$

and only the last of these terms cannot be determined immediately. However, on multiplying (A 23) by  $sI_0$  and rearranging, it can be shown that

$$\frac{d}{ds} \left[ sI_0 \frac{d \hat{C}_1}{ds} - sI_1 \hat{C}_1 \right] = sI_0 f,$$

so that, on integrating,

$$\hat{C}_1(p^\dagger) = - \frac{1}{p^\dagger I_1(p^\dagger)} \int_0^{p^\dagger} sI_0 f ds. \quad (\text{A } 27)$$

On performing the integrations in (A 25), (A 26) and (A 27) it follows eventually that

$$\hat{\Theta} = \left\{ \frac{4}{3p^3} + \frac{160}{3p^4} - \frac{4352}{3p^5} - \frac{10240}{p^6} + \left( \frac{512}{3p^8} + \frac{5120}{p^{11}} \right) \frac{I_0(p^\dagger)}{I_1(p^\dagger)} - \frac{128}{3p^4} \left[ \frac{I_0(p^\dagger)}{I_1(p^\dagger)} \right]^2 \right\} \quad (\text{A } 28)$$

( $\Theta \equiv \Sigma^2 + \mu^2$ ). The exact inverse of (A 28) is

$$\Sigma^2 + \mu^2 = \left\{ T^2 - \frac{1}{2^{\frac{1}{8}} 8} + \frac{512}{3} \sum_{n=1}^{\infty} \left( \frac{5}{\alpha_n^8} - \frac{60}{\alpha_n^{10}} + \frac{T}{\alpha_n^6} \right) \exp(-\alpha_n^2 T) \right\}, \quad (\text{A } 29)$$

so that  $\Sigma^2$  can be determined exactly using (A 18). However to obtain an expression useful for  $T \ll 1$ , (A 28) is inverted directly in the manner described following (A 18) to give (using (A 19) for  $\mu$ )

$$\Sigma^2 \approx T^2 \left\{ \frac{2}{9} - \frac{32}{9} T + \frac{13312}{315\pi^{\frac{1}{2}}} T^{\frac{3}{2}} - \frac{256}{3} T^2 + \dots \right\}. \quad (\text{A } 30)$$

This verifies the correctness of (2.25) but also shows that the coefficients of  $T^{\frac{3}{2}}$  and  $T^2$  are large, as noted in the paper.

The values of  $\mu$  and  $\Sigma^2 + \mu^2$  for case *C* can be obtained immediately from the corresponding results for cases *A* and *B*, when it is noted from (2.20)–(2.22) that  $F$  for case *C* is twice  $F$  for case *A* minus  $F$  for case *B*, and that the equation for *C* is linear. In particular it follows that for  $T \ll 1$

$$\left. \begin{aligned} \mu &\approx T \left\{ \frac{4}{3} - 4T + \frac{256}{15\pi^{\frac{1}{2}}} T^{\frac{3}{2}} - 8T^2 + \dots \right\}, \\ \Sigma^2 &\approx T^2 \left\{ \frac{2}{9} + \frac{32}{9} T - \frac{2048}{45\pi^{\frac{1}{2}}} T^{\frac{3}{2}} + 56T^2 + \dots \right\}, \end{aligned} \right\} \quad (\text{A } 31)$$

and, as in cases *A* and *B*, these have the properties in the paper.

From the exact expressions derived in this appendix it can be shown that for large  $T$  (which means for practical purposes that  $T$  must be greater than about 0.25) the values of  $\mu$  and  $\Sigma^2$  are given by

$$\left. \begin{aligned} \mu &= T, & \Sigma^2 &\approx \frac{1}{24} \left( T - \frac{1}{15} \right) & (\text{case } A), \\ \mu &\approx T - \frac{1}{48}, & \Sigma^2 &\approx \frac{1}{24} \left( T - \frac{3}{32} \right) & (\text{case } B), \\ \mu &\approx T + \frac{1}{48}, & \Sigma^2 &\approx \frac{1}{24} \left( T - \frac{29}{480} \right) & (\text{case } C). \end{aligned} \right\} \quad (\text{A } 32)$$

Thus the results are consistent with the work by Taylor (1953) and Aris (1956), but show that the initial distribution  $\mu$  affects the corrections to the leading terms predicted in these papers, in agreement with Chatwin (1970).

#### REFERENCES

- ARIS, R. 1956 On the dispersion of a solute in a fluid flowing through a tube. *Proc. Roy. Soc. A* **235**, 67.
- CHATWIN, P. C. 1970 The approach to normality of the concentration distribution of solute in a solvent flowing along a straight pipe. *J. Fluid Mech.* **43**, 321.
- CHATWIN, P. C. 1976 The initial dispersion of contaminant in Poiseuille flow and the smoothing of the snout. *J. Fluid Mech.* **77**, 593.
- JEANS, J. 1960 *The Kinetic Theory of Gases*. Cambridge University Press.
- LIGHTHILL, M. J. 1966 Initial development of diffusion in Poiseuille flow. *J. Inst. Math. Appl.* **2**, 97.
- SAFFMAN, P. G. 1960 On the effect of the molecular diffusivity in turbulent diffusion. *J. Fluid Mech.* **8**, 273.
- TAYLOR, G. I. 1921 Diffusion by continuous movements. *Proc. Lond. Math. Soc.* **20**, 196.
- TAYLOR, G. I. 1953 Dispersion of soluble matter in solvent flowing slowly through a tube. *Proc. Roy. Soc. A* **219**, 186.